International Journal of Hydrogen Energy 205 (2026) 153196

Contents lists available at ScienceDirect

International Journal of Hydrogen Energy

journal homepage: www.elsevier.com/locate/he

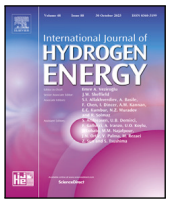

Comparing the safety of bunkering LH_2 and LNG using quantitative risk assessment with a focus on ignition hazards—Sensitivity analysis

Jorgen Depken [a,*], Lars Baetcke [a], Martin Kaltschmitt [b], Sören Ehlers [a]

[a] Institute of Maritime Technologies and Propulsion Systems, German Aerospace Center (DLR), Dünebergerstraße 108, Geesthacht, 21502, Schleswig-Holstein, Germany

[b] Institute of Environmental Technology and Energy Economics (IUE), Hamburg University of Technology (TUHH), Eissendorfer Strasse 40, Hamburg, 21073, Germany

ARTICLE INFO

Keywords:
Safety
Bunkering
Hydrogen
QRA
Shipping
LNG

ABSTRACT

Hydrogen, in its various storage forms, represents a potential fuel for climate-neutral shipping. In order to evaluate the safety of bunkering liquid hydrogen and to establish a basis for a comparison with the bunkering of LNG, a quantitative risk assessment has been conducted. This paper continues this work, by first realizing a quantitative risk assessment (QRA) with adopted systems allowing for the same bunkering duration for both fuels. The investigation shows that the diameter of the pipe has a significant impact on the frequency of hazardous events. To gain a deeper understanding of the effect, a sensitivity analysis is conducted. In addition to the frequencies, a notable impact of the pipe diameter can also be observed with regards to the safety distance in the full rupture case. Furthermore, the safety distances are found to be significantly impacted by wind speed and release time. The ambient temperature and humidity are identified to have only a minor impact.

1. Introduction

Although maritime transportation is currently the most efficient method of transporting goods, it is nevertheless necessary to reduce emissions in order to achieve the goals set out in the Paris Agreement and to prevent global warming from exceeding 2 °C. Presently, approximately 80 % of global trade is conducted via maritime transportation [1], with the shipping industry accounting for approximately 3 % of global CO_2-emissions [2]. It is evident that optimization of energy efficiency alone will not be sufficient to achieve the objectives defined within the Paris agreement [3]. Thus, novel and greenhouse gas (GHG) neutral fuels must be introduced into the maritime industry. In previous years, the international shipping industry has focused on LNG as an alternative fuel [4]. However, since LNG is still a fossil fuel, attention has shifted to "green" methanol, "green" ammonia and "green" hydrogen [4–6]. Due to the physical–chemical properties of these various "green" energy carrier the former two options are proposed more for longer distances while the latter is typically discussed in relation to smaller units and shorter distances. Hydrogen can be stored in different forms, for example, compressed in vessels with more than 200 bar or liquefied at roughly 20 K; due to spatial limits on ships the latter option is most widely discussed. But the low temperature of liquefied hydrogen and its high flammability present unique challenges to the safety of liquid hydrogen utilization in shipping.

1.1. Motivation and outline

The safety of a bunkering operation is of particular importance, given the inherent challenges associated with this type of activity. In [7] a comparison of the safety of bunkering liquid hydrogen and LNG has been performed, given that both fuels are flammable gases liquefied at cryogenic temperatures. A Quantitative Risk Assessment (QRA) was employed for the purpose of comparison. The same bunker system, comprising the same pipe and equipment with an identical diameter, was subjected to analysis. The different densities of the two fuels under investigation resulted in different transfer rates, which in turn yielded different bunker durations. It was found, that the bunker duration for liquid hydrogen (LH_2) was six times longer than that for LNG [7]. In accordance with the aforementioned bunker duration, the overall leak frequency was also six times higher for LH_2. The frequencies of the hazardous events of LH2 were larger by factors between 4.6 and 10. A consequence analysis was conducted, which revealed that liquefied natural gas (LNG) necessitates larger safety distances for the pool fire and explosion scenario. Conversely, liquefied hydrogen (LH_2) required larger safety distances in the event of a flash fire. Given that the flash fire necessitated larger safety distances than the other hazardous events, LH_2 requires the largest safety distances.

* Corresponding author.
E-mail address: jorgen.depken@dlr.de (J. Depken).

https://doi.org/10.1016/j.ijhydene.2025.153196
Received 20 January 2025; Received in revised form 7 November 2025; Accepted 22 December 2025
Available online 6 January 2026

This paper continues this research [7] by adapting the LH_2 system in a way that the bunker durations for both liquid gases are approximately equivalent. A new Quantitative Risk Assessment (QRA), following the methodology described in [7], is conducted with this newly defined system. To gain a deeper understanding of the factors influencing the results of such a QRA, additionally a sensitivity analysis is conducted and discussed.

This paper is therefore structured into five sections. The introduction provides an overview of the various bunkering methods and a summary of the current status of bunkering safety research. Subsequently, the employed methods for the QRA are briefly introduced, and methodological changes made compared to [7] are discussed. The system employed within this study is introduced and the methodology for the sensitivity analysis is outlined. The detailed results of the QRA and the sensitivity analysis are subsequently presented, and finally a conclusion is drawn.

1.2. Bunkering methods

The various bunkering methods are illustrated in Fig. 1. The aforementioned methods are independent of the fuel that is bunkered; however, it is possible that some may be more suitable for a specific fuel than others.

- The most prevalent method is ship-to-ship bunkering (Fig. 1(a)), whereby the fuel is supplied from a bunkering vessel to the receiving vessel. This method permits the transfer of substantial quantities of fuel at high flow rates. As the fuel supply to the ship is conducted from the sea side, cargo operations are typically not impeded, thereby enabling simultaneous operations [8].
- In the case of truck-to-ship bunkering (Fig. 1(b)), the fuel is transported to the quayside by a truck or semi-trailer. Then it is transferred to the ship using equipment attached to the trailer. Consequently, the transfer rate is constrained and the volume of fuel available to the ship is defined by the truck capacity. Furthermore, the presence of the truck on the quayside can impede the simultaneous execution of loading operations. Therefore, truck-to-ship bunkering is typically employed for smaller units [8].
- Shore-to-ship bunkering (Fig. 1(c)), also referred to as port-to-ship or terminal-to-ship bunkering, allows for the transfer of high flow rates and high volumes of fuel. However, the receiving vessel must be docked to the landside terminal, which restricts the possibility of conducting simultaneous cargo operations. Consequently, it is a relatively uncommon method [9].
- Container-to-ship bunkering (Fig. 1(d)) is not a conventional bunkering method, as it does not entail the transfer of fuel from one tank to another. Here, interchangeable tanks containing the fuel are loaded onto the ship and subsequently connected to the propulsion system (i.e., a cassette-type fuel system). Thus, when the tank is empty, the entire tank is replaced. Typically, ISO container frames should be used for convenient handling. Existing port infrastructure, such as cranes, can be employed to exchange the tanks allowing this method to be utilized in nearly every port. However, during the exchange of the tanks, the cranes are obviously not available for cargo operations, which extends the time the ship spends in port [10].

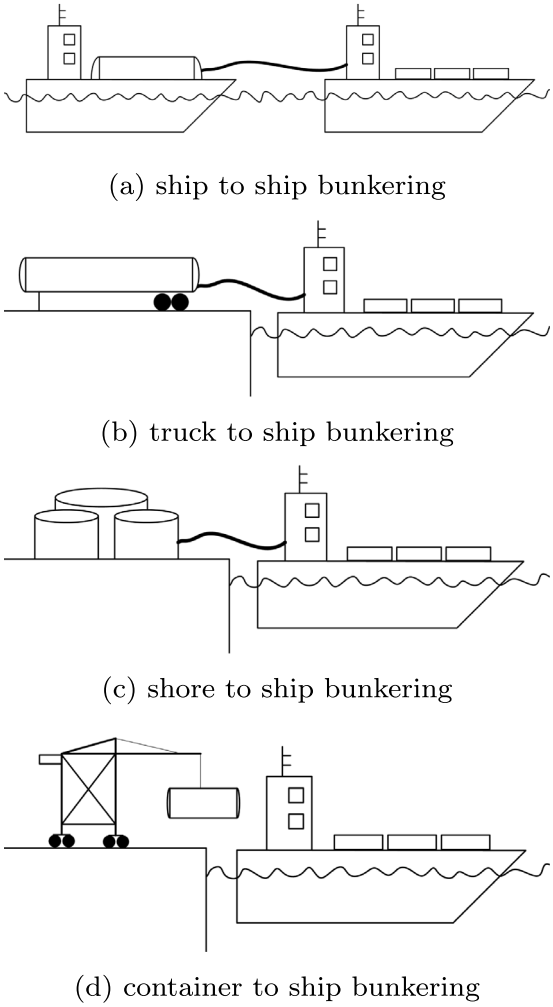

Fig. 1. Bunkering methods.

1.3. Current status of bunkering safety research

In light of the inherent dangers associated with bunkering, research has been conducted with the aim of enhancing its safety. However, the existing knowledge remains limited, particularly with regard to hydrogen as a novel fuel. With regard to LNG bunkering, a review of risk analysis methodology for simultaneous operations has been published by Fan et al. [11], while a review of ship-to-ship LNG bunkering has been published by Duong et al. [12]. A comparative analysis of safety zones due to dispersion was conducted for LNG and ammonia by Duong et al. [13].

Fan et al. [14] compared the evaporation and dispersion of LNG, LH_2 and ammonia for accidental releases during bunkering. A simple analytical relationship was chosen for the evaporation comparison, while a CFD analysis was created for the dispersion comparison.

Saborit et al. [15] considered the value chain of offshore hydrogen production, transport to the port, and then bunkering, analyzing each stage in turn. Aneziris et al. [16] employed a quantitative method to assess the safety of LNG ship-to-ship bunkering in a Greek port. Lee et al. compared the different bunkering methods (outlined in Section 1.2) by means of an analytical hierarchy process to determine the optimal method for a shipyard [8].

Zanobetti et al. [17] employed a multi-objective approach to compare four different onboard carbon capture and storage (OCCS) systems to a conventional LNG powertrain, an ammonia (NH_3) solid-oxide fuel cell (SOFC) powertrain and a liquid hydrogen proton-exchange membrane fuel cell (PEMFC) system. The LH_2 system has been identified to offer greater advantages than the onboard carbon capturing and storage (OCCS) system in terms of the volume occupied onboard, net present cost and global warming impact. In terms of safety, however, the OCCS system is to be preferred over the LH_2 or NH_3 systems. The NH_3 system occupied a smaller volume on board compared to the LH_2 system.

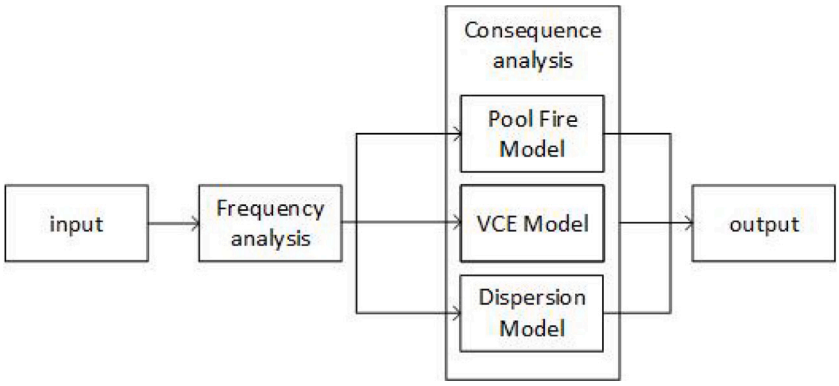

Fig. 2. Flow diagram of the QRA methodology.

Nevertheless, the LH_2 system was found to be more economically and safely advantageous than the NH_3 system. A quantitative methodology was also utilized for the purpose of comparing the safety of the two systems.

Klebanoff et al. [18] compared the physical and combustion properties of LH_2 and LNG with a focus on a cryogenic release and subsequent pool fire in a context of a high-speed ferry operating in the Say Francisco Bay. The study came to the conclusion, that the physical and combustion properties, and thus the risk, of LH_2 and LNG are very similar.

Tofalos et al. [19] employed a Quantitative Risk Assessment (QRA) for the purpose of comparing the safety of bunkering LH_2 and LNG, focusing on the ship-side bunker system. Jeong et al. [20] established the use of a QRA for the purpose of establishing safety zones for LNG bunkering.

A sensitivity analysis has not yet been conducted for a Quantitative Risk Assessment. This paper aims to fill this gap and provide a deeper understanding on the factors influencing the results of such a Quantitative Risk Assessment (QRA).

2. Methodology

Due to the fact that the methodology has been described in detail in [7], this section will commence with a brief summary of the applied method and then proceed to elucidate the modifications compared to [7] and the conducted sensitivity analysis.

The methodology employed for a comparison of safety was initially introduced by Tofalos et al. [19] and has been further developed in [7]. It is illustrated in Fig. 2.

2.1. Frequency analysis

The initial step is to follow an event tree (e.g., Jeong [21]) in order to obtain the frequencies of hazardous events. This event tree is illustrated in Fig. 3. The event tree [7,21] yielded three hazardous events: a pool fire, a flash fire and a vapor cloud explosion.

The initial leak frequency is obtained using a method established by the International Association of Oil & Gas Producers (IOGP) based on the UK Hydrocarbon Release Database [22].

In order to calculate the ignition probabilities, the Energy Institute model [23] was employed, calculating ignition probabilities for 28 environmental conditions. It assumed, that the probability for direct ignition is always 0.001. This probability had to be subtracted from the overall modeled ignition probability to obtain the probability for delayed ignition. For this study case number 5 “small plant gas LPG” is selected as the most accurate [7]. The formulae for this case are described in Table 1.

Each step of the event tree is then combined with the initial leak frequency to a frequency of the hazardous event. In general, a frequency of a hazardous event of 10^{-6} is accepted as the individual risk per annum (IRPA) [24,25]. This indicates that the risk of a lethal accident for an individual can be as high as 10^{-6} without the necessity for additional safety measures such as a safety distance.

Table 1
Ignition probabilities according to Energy Institute model.

Case no.	Case description	Release rate range (kg/s)	Equation
5	Small Plant Gas LPG	0.1–1	$P_{ign} = 0.00250 \cdot Q^{0.357}$
		1–3	$P_{ign} = 0.00250 \cdot Q^{1.568}$
		3–498	$P_{ign} = 0.00624 \cdot Q^{0.735}$
		> 498	$P_{ign} = 0.600$

Additionally, the social risk can also be considered. An accident with a high number of fatalities is generally perceived as being less socially acceptable than a series of accidents with a single fatality each. This is the case even if the total number of fatalities remains constant. As the social risk requires detailed knowledge about the surroundings, which are not known for this hypothetical case, it is beyond the scope of this paper.

2.2. Consequence analysis

Subsequently, the dispersion of the fuel in the flash fire case is then calculated using a Gaussian model according to [26]. This Gaussian model is employed due to its minimal computational requirements, despite its lack of accuracy. Here, a simplified version of the Gaussian model only considering the direct downwind direction (x-direction) is employed (Eq. (1)).

$$C(x,0,0) = \frac{Q_L}{\pi u_w \sigma_y \sigma_z} \tag{1}$$

$C(x,0,0)$: Concentration at some point in space in kg/m^3; u_w: wind speed in m/s (here 5 m/s); σ_y and σ_z: dispersion constants as functions of the distance and the wind stability class, in m;

The dispersion constants σ_y and σ_z (both in m) can be calculated using Eqs. (2) and (3).

$$\sigma_y = 0.04 \cdot R_d \cdot (1 + 0.0001 \cdot R_d)^{-0.5} \tag{2}$$

$$\sigma_z = 0.016 \cdot R_d \cdot (1 + 0.0003 \cdot R_d)^{-1} \tag{3}$$

In order to calculate the consequences from a vapor cloud explosion the TNT equivalent model was employed. As the name indicates, the equivalent mass of TNT, which can be derived from the available quantity of gas as illustrated in Eq. (4) [27], was used to calculate the overpressure caused by the vapor cloud explosion.

$$W_{TNT} = \frac{m_v \eta \Delta H_{c(gas)}}{\Delta H_{c(TNT)}} \tag{4}$$

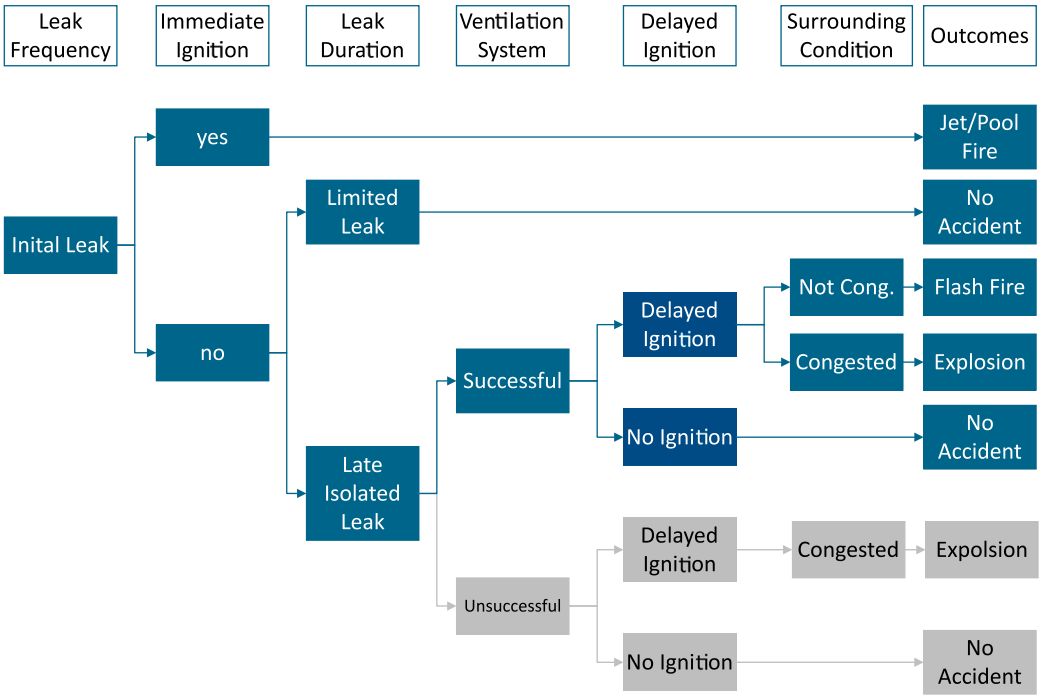

Fig. 3. Event tree used for frequency analysis ©CC-BY [7].

W_{TNT}: equivalent mass of TNT; m_v: total mass of flammable gas; η: explosion yield (= 0.1); $\Delta H_{c(gas)}$: lower heat of combustion of gas; $\Delta H_{c(TNT)}$: lower heat of combustion of TNT (= 4680 kJ/kg);

The scaled distance Z was then calculated by Eq. (5) [27].

$$Z = \frac{R_d}{W_{TNT}^{1/3}} \tag{5}$$

Z: scaled distance;

The scaled distance can be converted into the overpressure by a graph (see [27]). Eq. (6) was an approximation of said graph [19].

$$P_S = 573 \cdot Z^{-1.685} \tag{6}$$

P_S: overpressure, in kPa;

The critical effect in the pool fire case is the heat radiation, which is calculated using the point source model [28] according to Eq. (7).

$$Q_{rad}(R_d) = \tau_{atm}\chi_R \frac{(\pi/4)D^2 C_b \Delta H_C}{4\pi R_d^2} \tag{7}$$

$Q_{rad}(R_d)$: radiation on an object at a distance R_d; χ_R: fraction of combustion energy released, that is radiated (0.045 for LH_2 and 0.22 for LNG); D: Diameter of the fire; $C_b = 10^{-3} \cdot \Delta H_c/\Delta H_v$ liquid mass combustion flow; ΔH_c lower heat of combustion; ΔH_v heat of vaporization.

The transmissivity of the atmosphere τ_{atm} is calculated with the saturation vapor pressure $P_{w,sat}$ (Eq. (9)) according to Eq. (8).

$$\tau_{atm} = 1.5092 - 0.0708 ln\left(R_d P_{w,sat}(T_a)\frac{RH}{100}\right) \tag{8}$$

τ_{atm} transmissivity of the atmosphere, dimensionless; R_d is the distance traveled, in m; $P_{w,sat}(T_a)$ is the saturation vapor pressure of water, in Pa, see Eq. (9); T_a is the atmospheric temperature, in K; RH is the relative humidity, in %;

$$P_{w,sat} = exp(25.897 - 5319.4/T_a) \tag{9}$$

$P_{w,sat}(T_a)$ is the saturation vapor pressure of water, in Pa; T_a is the atmospheric temperature, in K;

The diameter of the pool is estimated by a simple heat balance. The heat input into the pool normalized to the surface area (see [29]) is illustrated in Table 2. The heat input is then compared to the heat of vaporization of the leaked fuel. The pool area is then calculated in the state of equilibrium by Eq. (10).

Table 2
Specific heat input into a pool of cryogenic liquid [29].

Heat input by	Heat source q [kW/m^2]	
	LH_2	LNG
Atmospheric convection	0.8	1.1
Radiation from flame	12	100-200
Radiation from ambient	1.6	1.6
Conduction from ground	100	9.2

$$A = \frac{Q_L \Delta H_V}{q_{cond} + q_{conv} + q_{rad} + q_{flame}} \tag{10}$$

A: area covered by the pool; Q_L: leak rate; ΔH_v heat of vaporization; q_{cond}, q_{conv}, q_{rad} and q_{flame} heat input into the pool, according to Table 2;

3. Frame conditions, definitions and data

In the following section the system employed in this analysis and the parameter considered during the sensitivity analysis are defined.

3.1. System definition

The system itself utilized in this paper is presented in Fig. 4 and is identical to that employed in [7]. Accordingly, the quantity of the installed equipment remains unaltered. The sole modification is another pipe and equipment diameter. The diameter of the LNG system is retained at 150 mm, while the diameter of the LH_2 system is increased to 350 mm. The diameter results in a bunker duration of 1:11 h for LNG and 1:06 h for LH_2. Consequently, the same amount of energy can be transferred to the ship. To achieve the same bunker duration, a technically hardly realizable diameter of 336.7 mm would be necessary. Thus, the diameter is rounded to the more practical 350 mm accepting

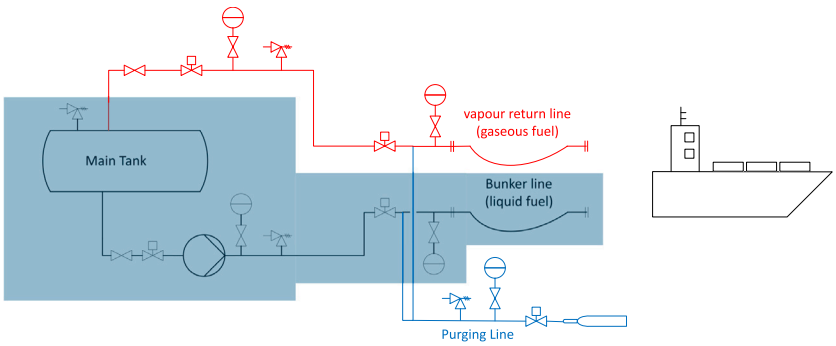

Fig. 4. Bunker system, the scope of this paper is highlighted in blue ©CC-BY [7].

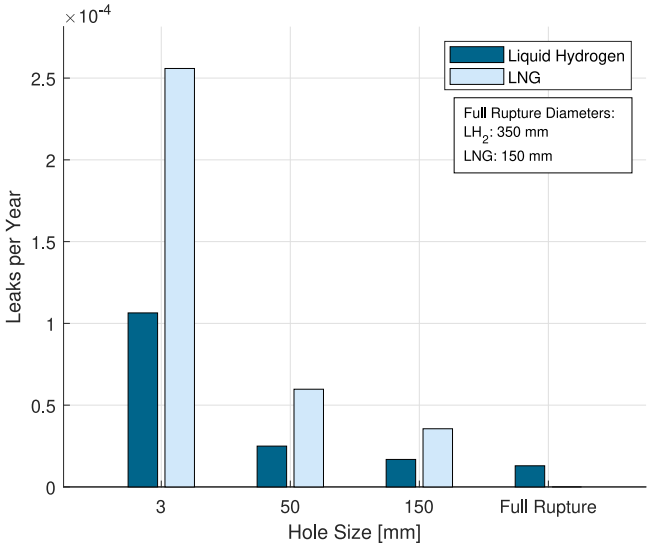

(a) Leaks per year of considered bunker system

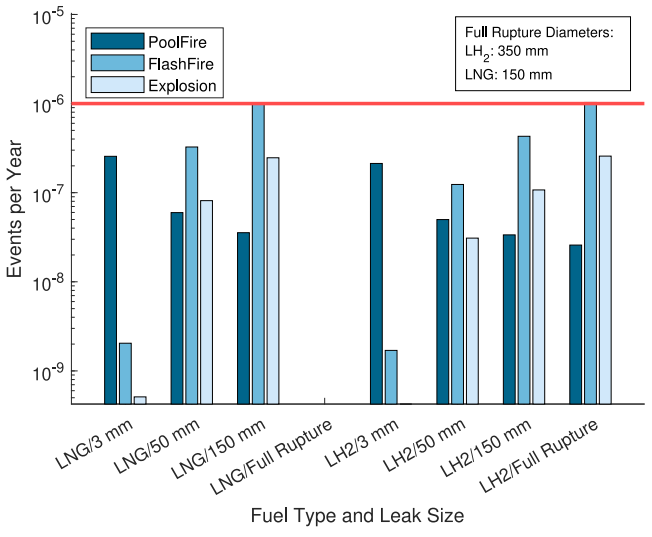

(b) Events per year of considered bunker system

Fig. 5. Results of frequency analysis.

a minor discrepancy in bunkering durations. The quantity and diameter of the equipment used in the LNG and LH_2 system is detailed in Table 3.

In addition to the leak diameters of 3, 50 and 150 mm, a 350 mm LH_2 leak is incorporated into the analysis to represent the full rupture case for this fuel.

Table 3
Equipment of bunkering system used in this paper.

Equipment	Count	Diameter (mm)	
		LNG	LH_2
Tank inlet	1	150	350
Pressure relieve valve	2	150	350
Pressure indicator	2	50	50
Pipes	10	150	350
Hose	30	150	350
Actuated valves	2	150	350
Manual valves	3	150	350
Flanges	17	150	350
Pump (centrifugal)	1	150	350

An ambient temperature of 10 °C and a wind speed of 5 m/s was chosen as atmospheric conditions being representative for Northern Germany. The relative humidity was set to 10 % to represent a worst case for the pool fire model.

Additionally, it was assumed that the safety mechanisms need a maximum of 30 s to stop a release. It was assumed, that 90 % of the leaks are limited and 10 % are late isolated leaks. Since bunkering is conducted on open deck, it was assumed, that the ventilation was always successful. It was assumed as well, that 80 % of the surrounding was not congested and 20 % was congested.

3.2. Sensitivity analysis

A sensitivity analysis is conducted for the four distinct phases of the Quantitative Risk Assessment (QRA), namely the frequency analysis, the vapor cloud explosion model, the pool fire model and the flash fire model. Subsequently, the model allows to analyze which parameters can be influenced and have an effect on the results. These parameters are listed in Table 4. With regard to the frequency analysis, the outcome is the leak frequency and the probabilities of the three hazardous events.

In the consequence analysis, the safety distance is the parameter of interest for the three models. As with the frequency analysis, the pipe diameter is investigated, but in contrast to that analysis, it represents only the full rupture case; other leak sizes are not considered. When the leak size remains constant, the amount of fuel released remains the same, and thus the consequence is the same. The parameters investigated for the consequence analysis can be found in Table 4.

4. Results and discussion

The following section presents the results of the Quantitative Risk Assessment (QRA), which are subsequently complemented by a sensitivity analysis.

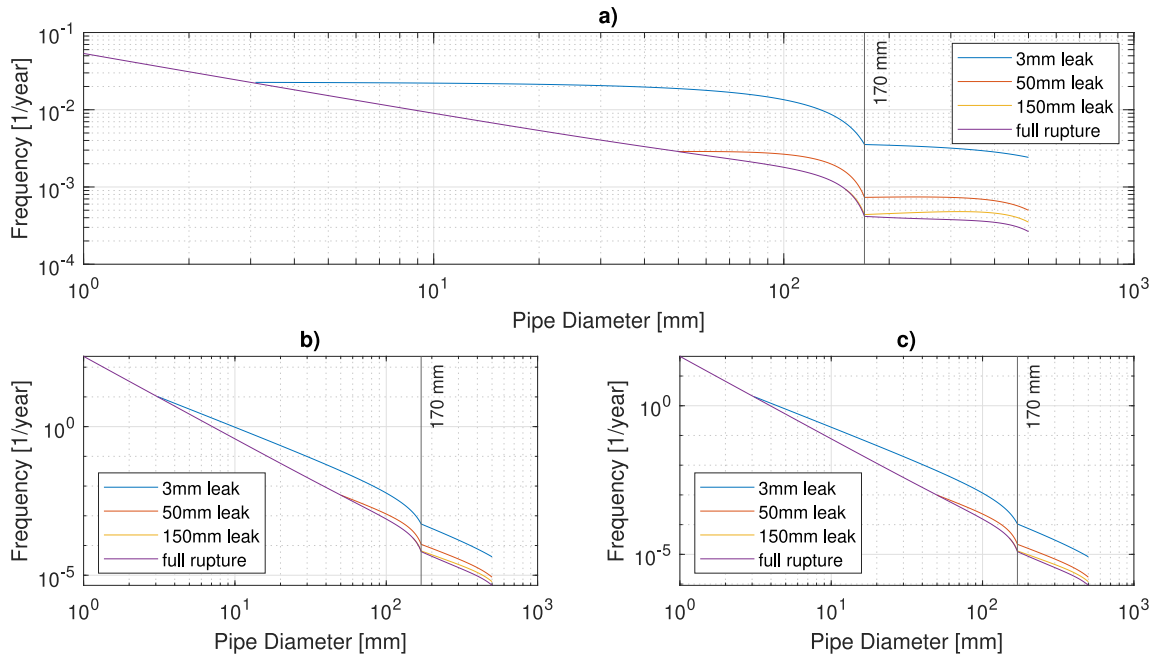

Fig. 6. Frequencies as function of pipe diameter (a) without considering the bunker duration, (b) considering the bunker duration of LH_2 and (c) considering the bunkering duration of LNG.

Table 4
Analyzed parameter in sensitivity analysis.

Model	Parameter	Variation range
Frequency analysis	Pipe diameter	1 mm–500 mm
Vapor cloud explosion	Pipe diameter	1 mm–500 mm
	Release time	1 s–300 s
Pool fire	Pipe diameter	1 mm–500 mm
	Humidity	5 %–100 %
	Ambient temperature	−10 °C–50 °C
Flash fire	Pipe diameter	1 mm–500 mm
	Wind speed	1 m/s–20 m/s

4.1. Quantitative risk assessment

The results of the conducted Quantitative Risk Assessment can be distilled into two principal findings: the frequencies of hazardous events and the requisite safety distances for each event. The results of the frequency analysis are given in Section 4.1.1 and those of the consequence analysis are given in Section 4.1.2.

4.1.1. Frequency analysis

The initial step is to conduct a frequency analysis. Fig. 5(a) presents the initial leak frequencies of both systems. Thus, hydrogen exhibits significantly lower frequencies than LNG, as larger pipes are less prone to leakage than smaller ones.

The initial leak frequencies presented in Fig. 5(a) are subsequently integrated with the ignition probabilities and other steps of the event tree (Fig. 5(b)). The IRPA of 10^{-6}, as described in Section 2, is indicated in Fig. 5(b) with a horizontal red line. Hydrogen displays elevated ignition probabilities in comparison to LNG, attributable to its high reactivity. This effect serves to counteract the lower leak frequencies of hydrogen to a certain extent. The outcome frequencies for hydrogen remain lower than those for LNG, even when the leak size is identical. The full rupture cases of both fuels are relatively comparable; however, a full rupture of hydrogen results in a leak of 350 mm, whereas a full rupture of LNG results in a leak of only 150 mm. A smaller leak releases a lesser quantity of fuel, thereby reducing the probability of ignition.

For a given leak size, the frequency of occurrence of incidents involving hydrogen is lower than that of incidents involving LNG. Nevertheless, the frequencies of the full rupture case are higher than those of LNG for two events, namely flash fire and explosion. The only event that exceeds the IRPA of 10^{-6} is the LH_2 full rupture flash fire.

4.1.2. Consequence analysis

The safety distances for the 3, 50 and 150 mm leak remain consistent with those previously established. As the leak size remains constant, the quantity of released fuel is also unaltered. The leakage rate is contingent upon the density of the released fuel. Consequently, LNG and LH_2 experience different release rates. Therefore, the effect of the fuel is also identical. As the LH_2 full rupture case is considerably larger than the one for LNG, it releases a greater quantity of fuel. Consequently, the larger amount of released fuel results in larger safety distances (see Table 5).

An increase in the leak diameters of LH_2 from 150 to 350 mm has been demonstrated to enhance the safety distances by approximately a factor of 2 for the pool fire and explosion case. Furthermore, the increase for the flash fire case is even more pronounced.

The results of the QRA demonstrate that the safety distances remain constant when the diameter of the leak and the quantity of released fuel remain unaltered. Conversely, the QRA demonstrates that increasing the pipe diameter to a value that yields equivalent bunker duration for both fuels reduces the frequencies of harmful events to a level below that which would be anticipated based on the reduced time. To gain further insights into the impact of these factors, a sensitivity analysis is subsequently performed.

4.2. Sensitivity analysis

As demonstrated in Section 4.1, the pipe diameter has a significant impact on the outcomes. In order to identify other parameters with a substantial impact, a sensitivity analysis is conducted.

4.2.1. Frequency analysis

Initially, the leak frequencies are examined as a function of the pipe diameter, with the results presented in Fig. 6. Fig. 6(a) illustrates the leak frequencies are shown for the full rupture case and leak sizes of 3 mm, 50 mm and 150 mm; the bunkering duration is so far not taken

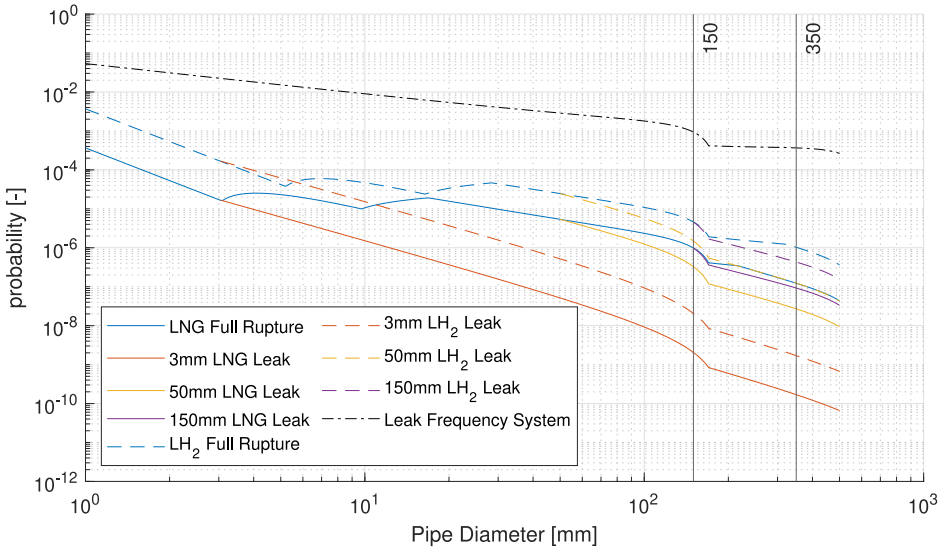

(a) Probability of a Flash Fire as a function of the pipe diameter

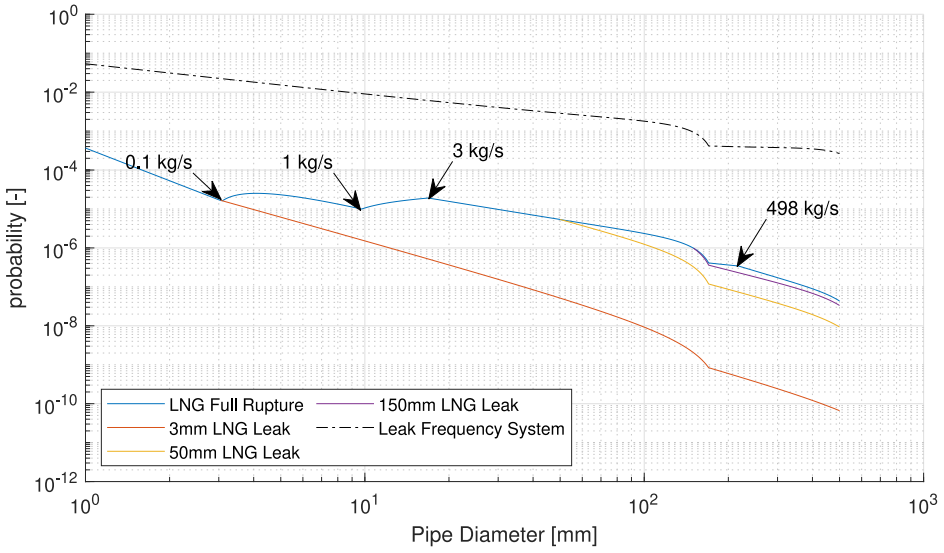

(b) Probability of a Flash Fire for LNG, the arrows indicate the changes in calculation of the ignition probability

Fig. 7. Probability of a flash fire.

Table 5
Safety distances of the considered system. The full rupture case is represented by the 150 mm leak for LNG and the 350 mm leak for LH_2.

Fuel	LeakSize	release rate	Safety distance for hazardous event		
			Pool fire	Explosion	Flash fire
LNG	3 mm	0.095 kg/s	1.2 m	4.1 m	16.3 m
	50 mm	26.4 kg/s	17.0 m	26.7 m	279.1 m
	150 mm	237.6 kg/s	49.0 m	55.5 m	922.0 m
LH_2	3 mm	0.033 kg/s	0.8 m	3.9 m	31.7 m
	50 mm	9.26 kg/s	11.0 m	25.2 m	575.7 m
	150 mm	83.31 kg/s	31.6 m	52.4 m	2108.0 m
	350 mm	453.6 kg/s	71.3 m	92.1 m	7701.8 m

into consideration. The model employs disparate functions to calculate the leak frequency above and below a diameter of approximately 170 mm. The precise point at which the function changes depend on the equipment type and varies in this case between 165 mm and 174 mm. Fig. 6 illustrates the average point of change in the function, which is indicated by a vertical line at 170 mm.

The bottom of Fig. 6 illustrates the leak frequencies when the bunkering duration is taken into account. Therefore, the bunkering duration has an influence solely on the gradient of the curve.

The initial leak frequencies illustrated in Fig. 6, when integrated with the remaining components of the event tree, facilitate the calculation of the probabilities associated with the three hazardous events. Fig. 7(a) illustrates the probability of a flash fire. Accordingly, the trajectory of the initial leak curve (represented in black) can be discerned within the flash fire probability curves (represented in color). However, additional inflection points are observable in the graph's progression. These are attributable to the specific ignition model employed. The Energy Institute Model [23] employs a distinct probability calculation methodology at release rates of 0.1, 1, 3 and 498 kg/s, indicated in Fig. 7(b) with arrows. Fig. 7(b) focuses on the curves for LNG, but the same is applicable for LH_2 as well. The inflection points occur exclusively in the full rupture case, as the release rate is no longer a variable, once the leak size is fixed. With a fixed release rate the ignition probability is also constant.

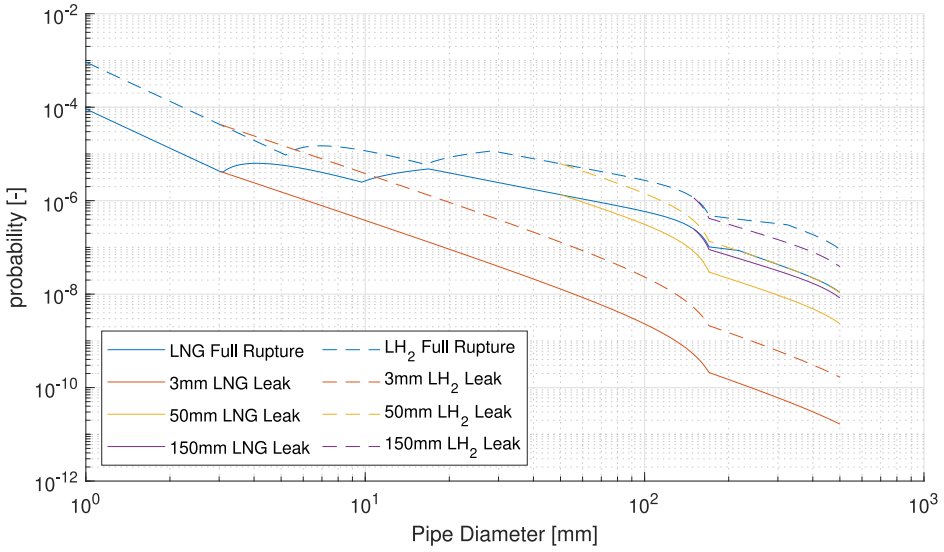

(a) Probability of an Explosion as a function of the pipe diameter

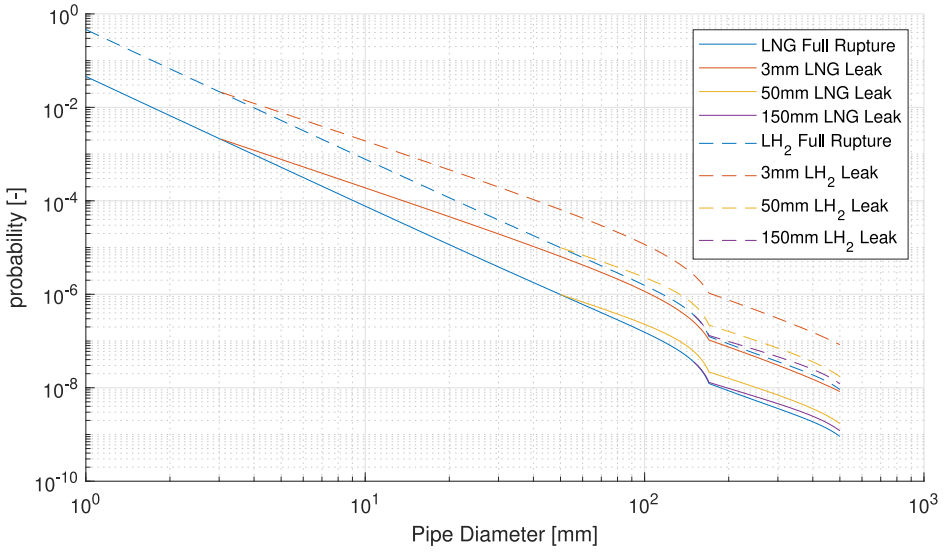

(b) Probability of a Pool Fire as a function of the pipe diameter

Fig. 8. Probabilities of an Explosion and a Pool fire as functions of the pipe diameter.

Fig. 8(a) illustrates the probability of an explosion as a function of pipe diameter. The distinction between Figs. 7(a) and 8(a) is the gradient of the curves, as the sole discrepancy between the two events in the event tree is the step of surrounding conditions. If the surrounding is congested, an explosion will occur. In the absence of congestion, a flash fire will occur. According to Section 2, it is assumed that 20 % of the surrounding area is congested and 80 % is not. This assumption is the source of the observed differences in gradient.

Fig. 8(b) illustrates the probability of a pool fire. In contrast to Figs. 7(a) and 8(a), no additional inflection points are evident in the curve. This is once more based on the Energy Institute Model [23] for the ignition probabilities. A flash fire and explosion are the result of a delayed ignition, whereas a pool fire is the result of an immediate ignition. According to the model, the probability of an immediate ignition was fixed at 0.001, as discussed in Section 2. The Energy Institute Model states that for highly reactive substances, such as hydrogen, this probability was doubled. Consequently, no inflection points in the curve occur; rather, the curves are only shifted.

A reduction in pipe diameter has been observed to result in a notable decrease in the frequency of both leaks and harmful events.

4.2.2. *Consequence analysis*

Subsequent to an investigation into the impact of pipe diameter on the probabilities of hazardous events and initial leak frequency, now factors influencing the safety distance are examined. Fig. 9 illustrates the impact of wind speed on the required safety distance for a flash fire. Even due to the fact that the employed model is not designed to simulate the release of large clouds of fuel, it is employed due to the unavailability of a more suitable alternative. As illustrated in Fig. 9, the lower wind speeds, approximately 5 m/s, are of greater relevance than the higher values. The wind probability 10 m above ground for the city of Hamburg based on historic data from 1950 to 2023 provided by the German Weather Service (Deutscher Wetterdienst, DWD) [30] is plotted in Fig. 9 in green. The impact of wind speed on dispersion is more pronounced at lower wind speeds, with a gradual decline at higher wind speeds. As the wind speed is the sole independent factor, no further factors were examined in the context of the flash fire case.

The greatest impact of the examined variables is observed in the context of wind speed in the flash fire case. An increase in wind speed from 1 to 20 m/s results in a reduction in safety distances by a factor of between 4.5 and 7.8, contingent on the dimensions of the leak and the type of fuel involved. The results indicate that larger

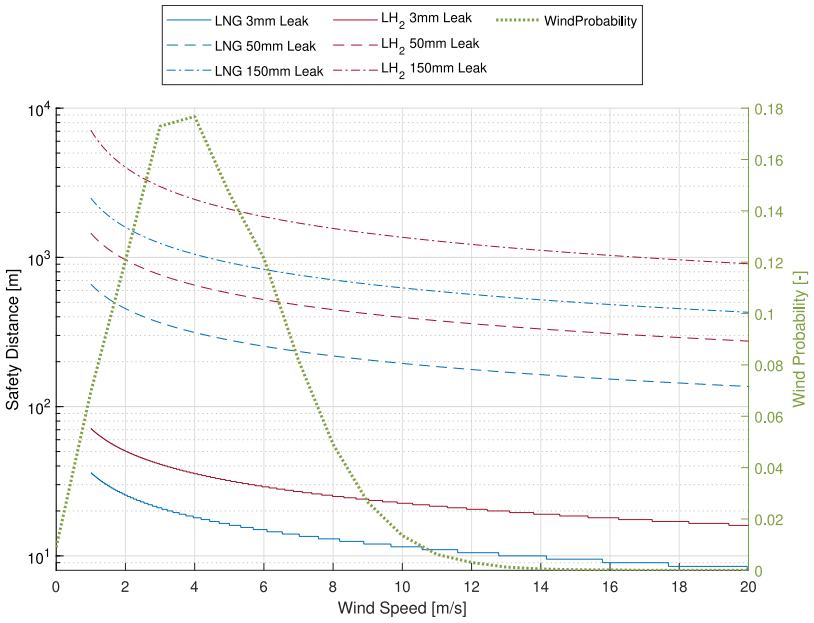

Fig. 9. Safety Distance Flash Fire as a function of wind speed and the probability of wind speed.

leaks result in a more pronounced reduction in the safety distance. The greatest alterations are observed in the context of low wind speeds. It is important to note that the Gaussian model employed in this QRA was not originally designed for large fuel releases and does not account for the buoyancy of fuels such as hydrogen or LNG. It is utilized primarily to reduce the computational time required for a CFD analysis; it was also selected as the most suitable alternative model for this purpose given the lack of other suitable models in the literature.

In order to calculate the requisite safety distance for the explosion case, the TNT equivalent model [27] (Section 2) was employed. In this calculation, the sole independent factor is the release time. Fig. 10 illustrates the safety distance for the explosion case as a function of the release time; i.e., the safety distance increases with the release time. The longer the fuel is released, the greater the quantity of fuel and, consequently, the greater the energy available for combustion in the explosion. This results in higher pressures from the explosion, necessitating larger safety distances.

The geometry of the congested space has an influence on the explosion; however, it is not considered in this hypothetical case due to the necessity of further assumptions. At a certain point, the congested space is entirely filled with fuel gas, which displaces oxygen from the space. This results in the upper flammability limit (UFL) being exceeded, which prevents the occurrence of an explosion. This effect is not included in the analysis presented here.

The second-largest effect is observed with regard to the release time in the explosion case. The safety distance increases by a factor of approximately 6.5 for all release rates and fuels when the release time is increased from 1 to 300 s. This is due to the possibility that the congested space may become completely filled with the fuel, resulting in the UFL being exceeded. In the absence of detailed knowledge of the surrounding environment, it is not possible to consider this effect.

In the pool fire model, two independent factors are examined: ambient temperature and humidity. The primary hazard associated with a pool fire is the heat radiation emitted by the fire. The absorption of radiation by humid air is greater than that of dry air, which consequently reduces the requisite safety distance. Fig. 11(a) illustrates the safety distance as a function of humidity. The influence of humidity is relatively minor in comparison to other factors, such as wind speed in the flash fire case. Similarly, cold air absorbs more radiation than warmer air. Fig. 11(b) illustrates the safety distance as a function of ambient temperature. Despite the dissimilarity in curve shape, the overall influence is of a comparable magnitude to that of humidity.

The safety distance is observed to remain relatively constant when the humidity and ambient temperature are varied for the pool fire case. An increase in temperature from −10 to 50 °C and humidity from 5 to 100 % results in a decrease in the safety distance of approximately 1.1.

4.2.3. Summary consequence models

The aforementioned results are summarized in Fig. 12(a), in which the corresponding maximum safety distance is normalized to the minimum value of each analysis. Fig. 12(a) illustrates that the wind speed in the flash fire case and the release time in the explosion case have a compatible impact on the outcome. In the flash fire case, a greater effect is observed for hydrogen than for LNG. Furthermore, wind speed has a more pronounced influence on larger release rates than on smaller ones. In the vapor cloud explosion case, the order of magnitude is consistent across all leak diameters and thus release rates. The aforementioned observations are very similar for LNG and LH_2. In the pool fire case, the investigated factors have a minimal influence, with the normalized safety distance approaching 1.

In the full rupture case, the pipe diameter also has an influence on the safety distance. The relationship between safety distances and pipe diameter is illustrated in Fig. 12(b). Thus, that the flash fire case necessitates the greatest safety distances of the three cases, exhibiting the most significant increase. As the pipe diameters increase the explosion and pool fire case converge. For smaller pipe diameters, the explosion case requires larger safety distances than the pool fire case. However, the pool fire case's safety distance increase is more pronounced, resulting in a gradual convergence.

An increase in pipe diameter for the full rupture case results in an augmented safety distance. In the flash fire case, the greatest safety distance is observed for all diameters. In the pool fire case, the safety distance exceeds that of the explosion case for the largest diameters; otherwise, the explosion necessitates larger safety distances.

4.3. Limitations

This study utilizes a quantitative risk assessment to comparatively analyze the safety of bunkering LNG and LH_2. The analysis thus concentrates on the primary hazards associated with the two fuels, namely

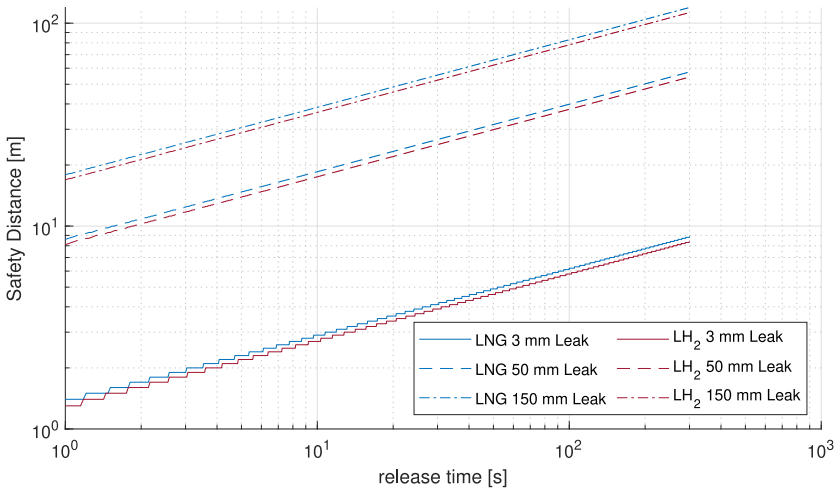

Fig. 10. Safety distance for explosion as function of release time.

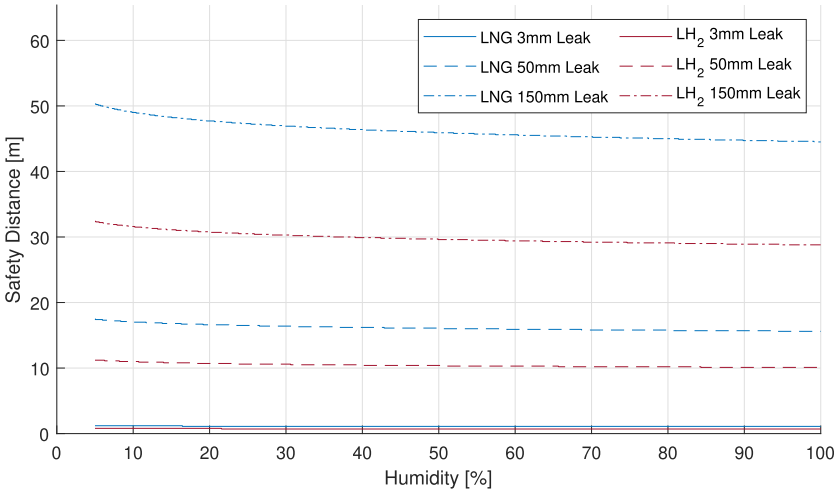

(a) Safety Distance Pool Fire as a function of humidity

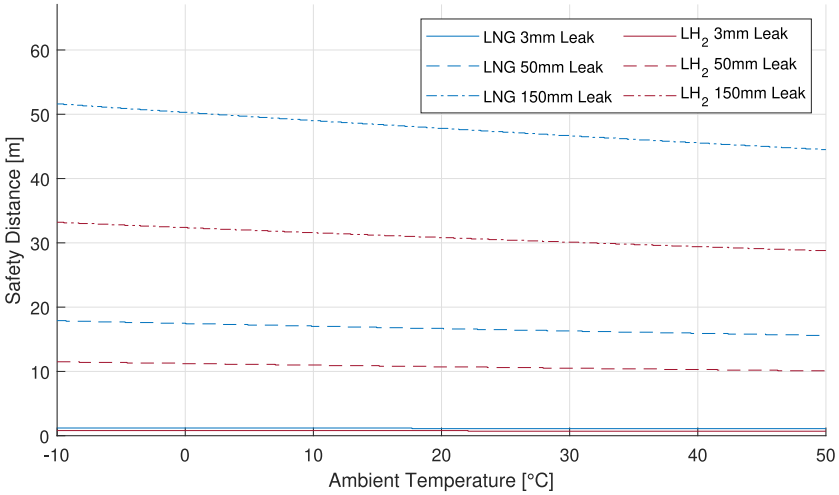

(b) Safety Distance Pool Fire as a function of ambient temperature

Fig. 11. Safety distance pool fire.

their flammability. This study does not address other potential hazards, such as temperature or asphyxiation.

The analysis deliberately excludes the safety subsystem, thereby isolating the comparison to the fuel characteristics alone. Furthermore, the modeling framework has been deliberately simplified to reduce computational overhead while still delivering robust and reliable outcomes. The system itself is also presented in a simplified version, as the objective of this study is to compare the fuels and not the systems.

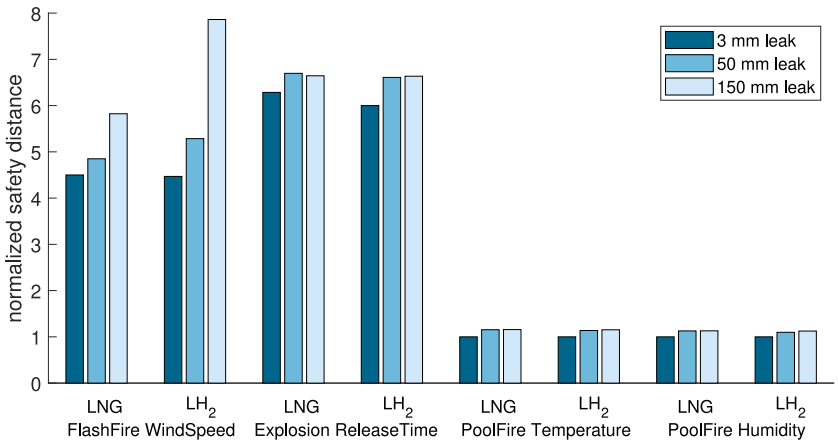

(a) normalized difference of safety distances

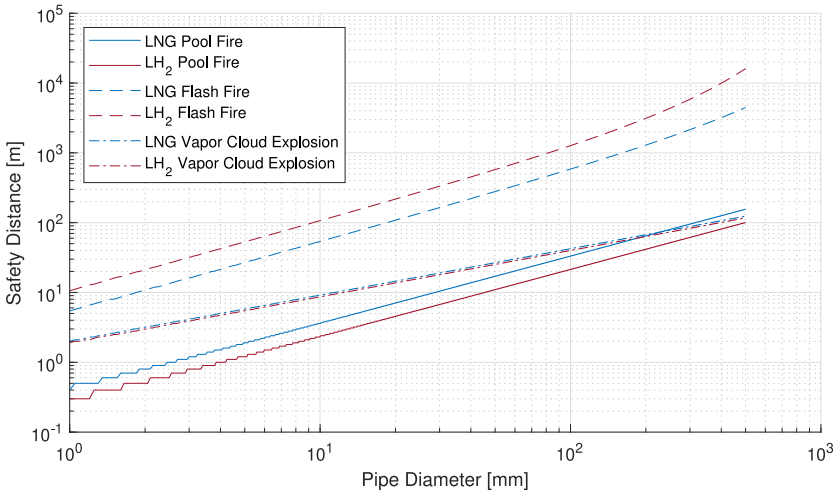

(b) safety distance as a function of the pipe diameter

Fig. 12. Results of sensitivity analysis of safety distance.

The integration of a more detailed system can be undertaken at a subsequent stage.

5. Conclusions

The following conclusions can be drawn:

- The pipe diameter has a significant effect on the leak frequencies. Nevertheless, the necessary safety distance for a full rupture increases with increasing system diameter. As a result of the increased pipe diameter, the frequency of hydrogen leaks is lower than that of LNG for the same leak diameter, as demonstrated in this analysis.
- The frequency of the full rupture case of both fuels (LNG: 150 mm; LH_2: 350 mm) is comparable , but hydrogen is slightly larger. The requisite safety distance for a given leak diameter is smaller for both explosion and pool fire cases involving hydrogen, and the safety distance for flash fires is smaller for LNG. A comparison of the full rupture cases for both fuels reveals that LH_2 necessitates the implementation of larger safety distances.
- The wind speed and the release time have a significant impact on the safety distance. It is imperative to exercise greater caution when selecting the wind speed for analysis and to implement measures to minimize the release time. However, the Gaussian dispersion model is not optimally suited for this analysis, necessitating further research into hydrogen dispersion.
- Ambient temperature and humidity have minimal influence on the safety distance for pool fires. Nevertheless, the employed pool model is a relatively rough estimation, designed to minimize computational requirements. This highlights a potential avenue for future work to enhance the accuracy of the model.

CRediT authorship contribution statement

Jorgen Depken: Writing – review & editing, Writing – original draft, Software, Project administration, Methodology, Investigation, Formal analysis, Conceptualization. **Lars Baetcke:** Writing – review & editing, Supervision. **Martin Kaltschmitt:** Writing – review & editing, Supervision. **Sören Ehlers:** Writing – review & editing, Supervision.

Declaration of competing interest

The authors declare that they have no known competing financial interests or personal relationships that could have appeared to influence the work reported in this paper.

Acknowledgments

The research leading to these results has been carried out under the framework of the project ”FuturePorts”. The project started in January 2022 and is led by the Program Directorate Transport within the German Aerospace Center (DLR), whose support we greatly appreciate.

References

[1] UNCTAD United Nations Conference on Trade and Development. Review of Maritime Transport 2019. New York, United States of America: UNCTAD United Nations Conference on Trade and Development; 2019, URL https://unctad.org/system/files/official-document/rmt2019_en.pdf,

[2] FABER J, Hanayama S, Zhang S, Pereda P, Comer B, Hauerhof E, van der Loeff WS, Smith T, Zhang Y, Kosaka H, Adachi M, Bonello J-M, Galbraith C, Gong Z, Hirata K, Hummels D, Kleijn A, Lee DS, Liu Y, Lucchesi A, Mao X, Muraoka E, Osipova L, Qian H, Rutherford D, de La Fuente SS, Yuan H, Perico CV, Wu L, Sun D, Yoo D-H, Xing H. Fourth IMO Greenhouse Gas Study 2020: Full Report. London, UK: International Maritime Organization; 2021.

[3] Xing H, Stuart C, Spence S, Chen H. Alternative fuel options for low carbon maritime transportation: Pathways to 2050. J Clean Prod 2021;297:126651. http://dx.doi.org/10.1016/j.jclepro.2021.126651.

[4] Ovrum E, Longva T, Leisner M, Bachmann Mehammer E, Gundersen Skåre O, Helgesen H, Endresen Ø. Energy Transition Outlook 2024 Maritime Forecast to 2050. Techreport, DNV; 2024, URL https://www.dnv.com/maritime-forecast.

[5] Balcombe P, Brierley J, Lewis C, Skatvedt L, Speirs J, Hawkes A, Staffell I. How to decarbonise international shipping: Options for fuels, technologies and policies. Energy Convers Manage 2019;182:72–88. http://dx.doi.org/10.1016/j.enconman.2018.12.080, URL https://www.sciencedirect.com/science/article/pii/S0196890418314250?via=ihub.

[6] Manias P, McKinlay C, Teagle DAH, Hudson D, Turnock S. A wind-to-wake approach for selecting future marine fuels and powertrains. Int J Hydrog Energy 2024;82:1039–50. http://dx.doi.org/10.1016/j.ijhydene.2024.07.377, URL https://www.sciencedirect.com/science/article/pii/S0360319924030659?via=ihub.

[7] Depken J, Simon-Schultz M, Baetcke L, Ehlers S. Comparing the safety of bunkering LH2 and LNG using quantitative risk assessment with a focus on ignition hazards. Int J Hydrog Energy 2024;83:1243–50. http://dx.doi.org/10.1016/j.ijhydene.2024.08.177.

[8] Lee Y-G, Kim J-K, Lee C-H. Analytic hierarchy process analysis for industrial application of LNG bunkering: A comparison of Japan and South Korea. Energies 2021;14(10):2965. http://dx.doi.org/10.3390/en14102965, URL https://www.mdpi.com/1996-1073/14/10/2965.

[9] Lee H, Choi J, Jung I, Lee S, Yoon S, Ryu B, Kang H. Effect of parameters on vapor generation in ship-to-ship liquefied natural gas bunkering. Appl Sci 2020;10(19):6861. http://dx.doi.org/10.3390/app10196861, URL https://www.mdpi.com/2076-3417/10/19/6861.

[10] Van Hoecke L, Laffineur L, Campe R, Perreault P, Verbruggen SW, Lenaerts S. Challenges in the use of hydrogen for maritime applications. Energy Environ Sci 2021;14(2):815–43. http://dx.doi.org/10.1039/d0ee01545h.

[11] Fan H, Enshaei H, Gamini Jayasinghe S. Safety philosophy and risk analysis methodology for LNG bunkering simultaneous operations (SIMOPs): A literature review. Saf Sci 2021;136:105150. http://dx.doi.org/10.1016/j.ssci.2020.105150.

[12] Duong PA, Ryu BR, Jung J, Kang H. A comprehensive review of the establishment of safety zones and quantitative risk analysis during ship-to-ship LNG bunkering. Energies 2024;17(2):512. http://dx.doi.org/10.3390/en17020512.

[13] Duong PA, Ryu BR, Jung J, Kang H. Comparative analysis on vapor cloud dispersion between LNG/liquid NH3 leakage on the ship to ship bunkering for establishing safety zones. J Loss Prev Process Ind 2023;85:105167. http://dx.doi.org/10.1016/j.jlp.2023.105167.

[14] Fan H, Xu X, Abdussamie N, Chen PS-L, Harris A. Comparative study of LNG, liquid hydrogen, and liquid ammonia post-release evaporation and dispersion during bunkering. Int J Hydrog Energy 2024;65:526–39. http://dx.doi.org/10.1016/j.ijhydene.2024.04.039, URL https://www.sciencedirect.com/science/article/pii/S0360319924012965?via=ihub.

[15] Saborit E, García-Rosales Vazquez E, Storch de Gracia Calvo MD, Rodado Nieto GM, Martínez Fondón P, Abánades A. Alternatives for transport, storage in port and bunkering systems for offshore energy to green hydrogen. Energies 2023;16(22):7467. http://dx.doi.org/10.3390/en16227467.

[16] Aneziris O, Koromila IA, Gerbec M, Nivolianitou Z, Salzano E. Ship-to-ship LNG bunkering: Risk assessment and safety zones. Chem Eng Trans 2022;2022(91):535–40. http://dx.doi.org/10.3303/CET2291090.

[17] Zanobetti F, Pio G, Bucelli M, Miani L, Jafarzadeh S, Cozzani V. Onboard carbon capture and storage (OCCS) for fossil fuel-based shipping: A sustainability assessment. J Clean Prod 2024;470:143343. http://dx.doi.org/10.1016/j.jclepro.2024.143343, URL https://www.sciencedirect.com/science/article/pii/S0959652624027926?via=ihub.

[18] Klebanoff L, Pratt J, LaFleur C. Comparison of the safety-related physical and combustion properties of liquid hydrogen and liquid natural gas in the context of the SF-BREEZE high-speed fuel-cell ferry. Int J Hydrog Energy 2017;42(1):757–74. http://dx.doi.org/10.1016/j.ijhydene.2016.11.024.

[19] Tofalos C, Jeong B, Jang H. Safety comparison analysis between LNG/LH_2 for bunkering operation. J Int Marit Saf Environ Aff Shipp 2020;4(4):135–50. http://dx.doi.org/10.1080/25725084.2020.1840859.

[20] Jeong B, Lee BS, Zhou P, Ha S-m. Evaluation of safety exclusion zone for LNG bunkering station on LNG-fuelled ships. J Mar Eng Technol 2017;16(3):121–44. http://dx.doi.org/10.1080/20464177.2017.1295786.

[21] Jeong B. (A thesis presented in fulfilment of the requirements for the degree of doctor of philosophy), Glasgow: Department of Naval Architecture, Ocean and Marine Engineering; June 2018, URL https://stax.strath.ac.uk/concern/theses/pg15bd88s.

[22] International Association of Oil & Gas Producers, editor. Process Release Frequencies: Risk Assessment Data Directory, Report 434-01. 2019.

[23] International Association of Oil & Gas Producers, editor. Ignition Probabilities: Risk Assessment Data Directory, Report 434-06. 2019.

[24] Quantitative Risk Assessment (QRA): An introduction to the quantitative assessment of risks associated with high hazard facilities. TÜV Rheinland Risktec; 2018, URL https://www.risktec.tuv.com/wp-content/uploads/2018/11/Risktec-QRA-brochure-i1.0-med-res-single-pages.pdf.

[25] IMO International Maritime Organization. Revised Guidelines For Formal Safety Assessment (Fsa) For Use In The IMO Rule-making Process: MSC-MEPC.2/Circ.12/Rev.2. 2018, URL https://wwwcdn.imo.org/localresources/en/OurWork/HumanElement/Documents/MSC-MEPC.2-Circ.12-Rev.2%20-%20Revised%20Guidelines%20For%20Formal%20Safety%20Assessment%20(Fsa)For%20Use%20In%20The%20Imo%20Rule-Making%20Proces...%20(Secretariat).pdf.

[26] Weiner RF, Matthews RA. Environmental engineering. 4th ed., updated ed.. Amsterdam: Butterworth-Heinemann; 2003, URL http://www.loc.gov/catdir/description/els031/2003050203.html.

[27] Lobato J, Rodríguez JF, Jiménez C, Llanos J, Nieto-Márquez A, Inarejos AM. Consequence analysis of an explosion by simple models: Texas refinery gasoline explosion case. Afinidad J Chem Eng Theor Appl Chem 2009;66. URL https://raco.cat/index.php/afinidad/article/view/279547.

[28] Raj PK. LNG fires: a review of experimental results, models and hazard prediction challenges. J Hazard Mater 2007;140(3):444–64. http://dx.doi.org/10.1016/j.jhazmat.2006.10.029.

[29] Verfondern K, Dienhart B. Pool spreading and vaporization of liquid hydrogen. Int J Hydrog Energy 2007;32(2):256–67. http://dx.doi.org/10.1016/j.ijhydene.2006.01.016.

[30] Deutscher Wetterdienst (DWD). Hourly mean value from station observations of wind speed and wind direction for Germany, Version v24.03. Deutscher Wetterdienst (DWD); 2024, URL https://opendata.dwd.de/climate_environment/CDC/observations_germany/climate/hourly/wind/historical/.